ELSEVIER

Biochemical Engineering Journal 3 (1999) 141–150

Biochemical Engineering Journal

Evaluating strategies for overcoming overheating problems during solid-state fermentation in packed bed bioreactors

Victoria M. Ashley, David A. Mitchell[1], Tony Howes*

Department of Chemical Engineering, The University of Queensland, Brisbane, Qld, 4072, Australia

Received 27 May 1998; accepted 20 January 1999

Abstract

Normal operation of packed bed bioreactors used for solid-state fermentation involves a static bed aerated from the bottom throughout the fermentation. This leads to axial temperature profiles with the highest temperature, sometimes over 20°C higher than the inlet air temperature, occurring at the top of the bed. An axial heat transfer model was used to explore two strategies designed to prevent the temperature reaching undesirable levels, namely periodic reversal of the direction of airflow, and periodic mixing. Simulations were done for the growth of *Aspergillus niger* on a starchy substrate. The bed was assumed to be wide enough such that the radial heat transfer could be ignored. With hourly air reversal or mixing events, the maximum temperature predicted during the fermentation is higher than the maximum temperature predicted for normal operation. Increasing the frequency of air reversals leads to temperatures close to the maximum for growth in the middle of the bed. However, for a 0.345 m high bed and a superficial air velocity of 0.0236 m s^{-1}, mixing 10–60 times per hour can lead to lower maximum temperatures in the column compared to normal operation, because the frequent mixing distributes the benefits of the effective cooling at the bottom of the column throughout the bed. The degree of reduction in maximum temperature increases with increasing specific growth rate of the microorganism. Modelling is a useful tool in guiding experimental programs for the design and scale-up of bioreactors for solid-state fermentation, since it can be used to identify promising strategies and eliminate unfruitful strategies.

Keywords: Solid-state fermentation; Packed bed bioreactor; Bioreactor operation; Mathematical modelling

1. Introduction

Solid-state fermentation (SSF) involves the growth of microorganisms on moist solid substrates in the absence of free water. This absence of free water makes SSF cultivation systems quite different from submerged liquid fermentation (SLF) systems. Due to the solid nature of the substrate, it is difficult to mix the substrate bed effectively, and as a result, significant gas, water and temperature gradients may be established across the bioreactor. As a result, SSF systems are more complex than most SLF systems. Unfortunately, compared to the extensive literature for SLF, little is known about how to design and operate large-scale bioreactors for SSF. This lack of knowledge limits the successful development of commercial scale SSF processes [1]. Mathematical models describing heat and mass transfer processes in SSF are essential for the effective design of large-scale bioreactors, but such models are currently lacking [2].

Packed bed bioreactors, which typically have static substrate beds, are suited to SSF processes in which mixing is deleterious, such as the production of fungal spores. They allow better control of fermentation parameters than is possible in trays. In large trays problems arise with high temperatures and lack of oxygen in the centre [3,4]. In packed beds these problems are partially overcome by forced aeration, but high temperatures can still be reached near the air outlet. Under some operating conditions, temperatures in the bed can be 20°C higher than the temperature of the inlet air, leading to large variations in growth and product formation [5].

Sangsurasak and Mitchell [6] used a mathematical model of heat transfer in a packed bed bioreactor to investigate the effects of the bed height and the temperature and flowrate of the air on the bioreactor performance. However, these manipulations were predicted to be only partially successful: they reduced axial temperature gradients but did not prevent them from being established. The present work investigates

*Corresponding author. Tel.: +61-7-3365-4262; fax: +61-7-3365-4199; e-mail: tonyh@cheque.uq.edu.au

[1]Current address: Departamento de Engenheira Quimica, Universidade Federal do Parana, Cx. P. 19011, 81531-970 Curitiba, Parana, Brazil.

1369-703X/99/$ – see front matter
PII: S1369-703X(99)00010-8

two further strategies, air reversal and periodic mixing, the idea being to reverse the direction of airflow or mix the column contents before the temperature near the air outlet reaches deleterious levels. Obviously mixing can only be used if it does not adversely affect the microorganism or the final form of the product. The model predicts that frequent mixing has some potential to decrease the maximum temperature obtained in a packed bed.

2. Model development

The system modelled is a cylindrical packed bed bioreactor, aerated from the bottom with moist air (Fig. 1). A moist starchy substrate is inoculated with *Aspergillus niger* and placed in the bioreactor at time zero. The model concentrates on the heat transfer phenomena. Equations for mass transfer have not been incorporated. Sangsurasak and Mitchell [7] described the development of a model which was identical except that it described heat transfer in both the vertical and horizontal directions. In the current work the bed is assumed to be wide enough such that heat transfer in the horizontal direction to the bioreactor walls makes a negligible contribution to the overall heat removal and is therefore ignored. Sangsurasak and Mitchell [7] discussed the other assumptions in the current model and since their model described the experimental data of Saucedo-Castaneda et al. [8] and Ghildyal et al. [5] well, the assumptions are accepted as reasonable and are not discussed here. Although this model is obviously a simplification of packed bed operation, it is still a useful tool for investigating the heat transfer dynamics of a packed bed under different operating conditions.

2.1. Growth kinetics

The growth kinetics are described empirically by the logistic equation:

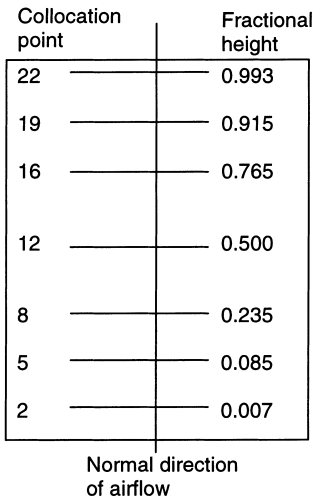

Fig. 1. Diagram of the column bioreactor, showing the fractional heights of collocation points 2, 5, 8, 12, 16, 19 and 22.

$$\frac{dX}{dt} = \mu_g . X\left(1 - \frac{X}{X_m}\right), \tag{1}$$

where X is the biomass concentration (kg biomass per kg dry matter) and X_m is the maximum possible biomass concentration. The specific growth rate μ_g (s^{-1}) is expressed empirically as a function of temperature [7]:

$$\mu_g = \mu_{gopt}, \quad T = T_{opt}, \tag{2a}$$

$$\mu_g = \left(\frac{b + (T_{max} - T_{opt})}{(T_{max} - T_{opt})}\right)\left(\frac{\mu_{gopt}(T_{max} - T)}{b + (T_{max} - T)}\right), \quad T_{opt} \le T \le T_{max}, \tag{2b}$$

$$\mu_g = 0, \quad T = T_{max}, \tag{2c}$$

where μ_{gopt} is the specific growth rate (s^{-1}) at the optimal temperature for growth (T_{opt}) and T_{max} is the maximum temperature at which growth can occur. The parameter b describes the sensitivity of the specific growth rate to increases in temperature [7].

2.2. Energy balance

Since heat transfer to the wall is considered negligible, only axial heat transfer is considered. Eq. (3) is the macroscopic energy balance over the column, including terms for convective and evaporative heat removal, conduction in the axial direction, and the generation of heat from microbial growth:

$$\rho_b C_{pb}\left(\frac{\partial T}{\partial t}\right) + (\rho_a C_{pa} + \rho_a f\lambda)v_z\left(\frac{\partial T}{\partial z}\right) = k_b\left(\frac{\partial^2 T}{\partial z^2}\right) + \rho_s(1-\varepsilon)Y\frac{dX}{dt}, \tag{3}$$

where each term has the units of W m^{-3}. Air moves only in the axial direction, with a constant velocity profile across the bed. The air and the moist solid at any particular location within the bed are assumed to be in thermal equilibrium, with the air saturated with water vapour. Of course the temperature and water content can vary with axial position. The factor $\rho_a f\lambda$ arises since the evaporation of water to keep the air saturated gives the air a higher apparent heat capacity [7]. The last term of the energy balance assumes that metabolic heat generation is directly proportional to the production of new biomass. Maintenance metabolism is ignored as are the effects of microbial growth on particle size and pressure drop across the bed.

Values for density, thermal conductivity and heat capacity of the bed were calculated as weighted averages of the properties of the air and substrate within the bed. Density and thermal conductivity were volume weighted, while heat capacity was mass-weighted:

$$\rho_b = \varepsilon.\rho_a + (1-\varepsilon)\rho_s, \tag{4a}$$

$$k_b = \varepsilon.k_a + (1-\varepsilon)k_s, \tag{4b}$$

$$C_{pb} = (\varepsilon\rho_a(C_{pa} + f.\lambda) + (1-\varepsilon)\rho_s C_{ps})/\rho_b. \tag{4c}$$

Implicit in these equations is the assumption that the thermal properties of the microorganism are equal to those of the substrate and that the void fraction does not change with time. Further knowledge of how these properties change during a fermentation is required before expressions describing such changes can be incorporated into a model.

2.3. Initial and boundary conditions

The boundary conditions are as follows:

$$z = 0, \quad T = T_a, \tag{5a}$$

$$z = H, \quad \frac{\partial T}{\partial z} = 0. \tag{5b}$$

These boundary conditions correspond to the bottom of the bed being maintained at the inlet air temperature (T_a) by the inlet air and the absence of external cooling at the top of the bed, with the air leaving the bed at the temperature of the top of the bed.

At the beginning of the fermentation both the initial temperature (T_0) and the inoculum concentration (X_0) are assumed to be constant over the whole height (H) of the bed:

$$\text{at } t = 0, \quad T = T_0, \quad 0 \le z \le H, \tag{6a}$$

$$\text{at } t = 0, \quad X = X_0, \quad 0 \le z \le H. \tag{6b}$$

2.4. Parameters

Table 1 lists parameters for the system [5,7–16]. The parameters were estimated by Sangsurasak and Mitchell [7] for the systems of Ghildyal et al. [5] and Saucedo-Castaneda et al. [8], both of whom grew *Aspergillus niger* on starchy substrates in packed bed bioreactors. A column height of 0.345 m, the same as that used by Ghildyal et al. [5], was used in the simulations.

Table 1
Parameter values used in the simulations with the mathematical model

Symbol	Value	Source
b	62.75	[7]
C_{pa}	1180 J kg^{-1}K^{-1}	[9]
C_{ps}	2500 J kg^{-1}K^{-1}	[10]
f	0.00246 kg water (kg air)$^{-1}$K^{-1}	[9]
k_a	0.0206 W m^{-1}K^{-1}	[11]
k_s	0.3 W m^{-1}K^{-1}	[12]
H	0.345 m	[5]
T_a	30°C=303 K	[5]
T_0	30°C=303 K	[5]
T_{opt}	35°C=308 K	[13]
T_{max}	52°C=325 K	[5]
X_0	0.001 kg biomass (kg dry matter)$^{-1}$	[8]
X_m	0.125 kg biomass (kg dry matter)$^{-1}$	[14]
v_z	0.0236 m s^{-1}	[5]
Y	8.366×10^6 J (kg biomass)$^{-1}$	[8]
ε	0.35	[15]
λ	2 414 300 J (kg water)$^{-1}$	[9]
μ_{gopt}	0.236 h^{-1}=6.56×10^{-5} s^{-1}	[13]
ρ_s	700 kg m^{-3}	[8]
ρ_a	1.14 kg m^{-3}	[16]

2.5. Computational methods

Orthogonal collocation was used to discretize the axial coordinate [17,18], leaving a set of ordinary differential equations. The equations were solved using the GEAR package [19]. Orthogonal collocation has difficulty in coping with physical situations involving advancing fronts, with both temporal and spatial oscillations arising in the predictions as a result of numerical instabilities. However, simulations with increasing numbers of collocation points showed that these oscillations could be minimized with 23 collocation points (including the two end points). The locations of some of these points are indicated in Fig. 1.

The numerical method calculates the temperature and biomass at each of the collocation points. These collocation points are not evenly spaced. Therefore, at each mixing time the average temperature was calculated as follows:

$$T_{avg} = \sum_{i=1}^{n+1} \left((Z_{i+1} - Z_i) \frac{(T_{i+1} + T_i)}{2} \right), \tag{7}$$

where T_i and Z_i are the temperature immediately prior to mixing and the fractional height of the ith collocation point, respectively. The average temperature (T_{avg}) was then assigned to all the collocation points. The same algorithm was also used to calculate the effect of mixing on the biomass concentration. This numerical strategy for representing mixing is equivalent to assuming instantaneous mixing of the bed.

For air reversals, when the direction of the airflow was changed so that the air entered at the top of the column, this was simulated by changing the sign on the superficial velocity and changing the boundary conditions to:

$$z = 0, \quad \frac{\partial T}{\partial z} = 0, \tag{8a}$$

$$z = H, \quad T = T_a. \tag{8b}$$

When the air inlet was switched back to the bottom of the column, the superficial velocity and boundary conditions were changed back to their original state.

2.6. Model of a well-mixed bed

For comparison, the system was also solved assuming that the bed was perfectly mixed throughout the fermentation. The air leaving the bed was assumed to be in thermal and moisture equilibrium with the bed, giving the following equation:

$$\rho_b C_{pb} \left(\frac{\partial T}{\partial t} \right) + (\rho_a C_{pa} + \rho_a f \lambda) \frac{v_z}{H} (T - T_a) = \rho_s (1 - \varepsilon) Y \frac{dX}{dt}. \tag{9}$$

Eq. (9) was solved using a fourth-order Runge–Kutta

algorithm, with the following initial conditions:

$$\text{at } t = 0, \quad T = T_0, \tag{10a}$$

$$\text{at } t = 0, \quad X = X_0. \tag{10b}$$

3. Results and discussion

The initial simulations and calculations involve separate treatment of the heat generation and heat removal phenomena within the packed bed system. An understanding of these underlying phenomena enables interpretation of the performance of the packed bed bioreactor during a fermentation.

In this work, it is assumed that it is undesirable for any part of the bioreactor to reach a temperature 5 K above the optimum temperature for growth. We refer to this as the critical temperature, and the column is said to have overheated if this critical temperature is exceeded in any part of the column during the fermentation. In actual fermentation the critical temperature might correspond to a temperature which triggers sporulation, or which has adverse effects on product formation. This simplified method of formulating the fermentation objectives with respect to temperature is used because the effects on growth of temporal variations in temperature during the fermentation are not clear [7]. Better knowledge of microbial responses to varying temperatures will allow the fermentation objectives to be formulated more precisely. However, in the absence of this knowledge, the concept of a critical temperature is sufficient for exploring column performance.

3.1. Characteristic heating time

The characteristic heating time is defined for the column as the time the system would take to increase in temperature by 5 K in the absence of all heat removal mechanisms. This 5 K rise corresponds to the difference between the optimum temperature of 308 K and the critical temperature of 313 K. The calculation is done at the time of the peak heat generation rate, which for logistic growth kinetics is when the biomass concentration is half of the final biomass concentration. It also assumes that the specific growth rate remains constant at μ_{gopt}. Under these conditions the heat generation rate (Q_{gen}) and the rate of heating of the bed (Q_{heat}) are:

$$Q_{gen} = 0.25\rho_s(1-\varepsilon)Y\mu_{gopt}X_m, \tag{11}$$

$$Q_{heat} = Q_{gen}/(\rho_b C_{pb}). \tag{12}$$

The bed values in the denominator of Eq. (12) are calculated according to Eqs. (4a) and (4c). Using the parameters listed in Table 1, Q_{gen} is equal to 7803 J s^{-1} m^{-3} and therefore Q_{heat} equals 0.00684 K s^{-1}. This corresponds to a temperature rise of approximately 0.4 K min^{-1}, and it would take approximately 12 min for the bed to heat by 5 K. In the absence of cooling, such heating would occur evenly along the length of the bed. The conclusion from this analysis is that the frequency of mixing or air reversal needs to be of the order of 10 min to have any chance of preventing overheating at the time of the peak heat generation rate. Note that if the strategy can cope with the peak heat load, it can cope throughout the fermentation.

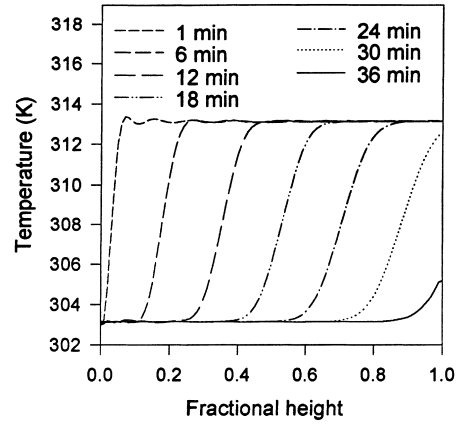

Fig. 2. Front behaviour in a column bioreactor in the absence of growth. The 0.345 m tall column is initially at a uniform temperature of 313 K. Air at 303 K is then blown into the column at a superficial velocity of 0.0236 m s^{-1}. The temperature profiles predicted within the bed are shown at various times.

3.2. Front behaviour

The convective cooling of the bed can also be analysed. The assumption of equilibrium between the solid and air phases leads to a situation analogous to convection alone, but with a higher apparent heat capacity of the air, due to the contribution of evaporation [7]. Although only the word convection is used in the discussion below, both processes are occurring.

This analysis is more complicated than the analysis of the characteristic heating time because the effectiveness of convective cooling is a function of axial position. However, the model can be used to characterize this behaviour. Fig. 2 shows the model predictions for cooling of the bed in the absence of microbial growth, with the initial bed temperature at the critical temperature and a superficial velocity of 0.0236 m s^{-1}, the highest value used by Ghildyal et al. [5]. The other parameters are as given in Table 1. Convective cooling under these conditions causes a temperature front to travel up the column. It takes over 24 min for any noticeable decrease in temperature to occur at the far end of the column, despite the fact that a parcel of air spends a fraction of a minute in the column. This can be explained as follows: as the first parcel of cool air enters the bed, heat is transferred to it from the substrate at the bottom of the bed, until the substrate and air are at thermal equilibrium. The air leaving the bottom of the bed is therefore warmer than the inlet air, but still cooler than the rest of the bed. However, as it progresses up the bed, it quickly warms to the initial temperature of the bed. Once this happens, it cannot

cool the remainder of the bed. The next parcel of air is warmed less by the bottom of the bed, which is now cooler than the initial bed temperature. Therefore, the next parcel of air travels a little further up the bed before it reaches the initial bed temperature. Since the air has a relatively small thermal mass compared to the substrate, it heats up from the inlet temperature to the initial bed temperature over a relatively small distance, which leads to the relatively sharp temperature front noted in Fig. 2. The front becomes less sharp over time due to the contribution of conduction to heat removal.

This analysis shows why the overheating problem occurs at the top of packed bed bioreactors when they are aerated from the bottom throughout the fermentation. The bottom of the column is cooled most effectively because it is in contact with cool air. Higher up in the column the air has been preheated by contact with the lower regions and therefore the bed is less effectively cooled, leading to higher temperatures being reached during the fermentation.

In this work the characteristic cooling time is defined as the time it takes for the far end of the column to cool by 5 K. In Fig. 2 it takes 27.5 min for the last collocation point in the bed (located at Z=0.993) to cool from 313 to 308 K. This characteristic cooling time will effectively be inversely proportional to the superficial velocity.

This analysis of the underlying heating and cooling effects suggests that overheating would be expected in a system characterized by the parameters listed in Table 1, and operated with simple bottom to top aeration throughout the fermentation, since the characteristic heating time is about one half of the characteristic cooling time. This is confirmed by the temperature profile for such operation shown in Fig. 3. Around the time of peak heat generation, the top 23% of the column is above the critical temperature, since collocation point 16, at Z=0.765, reaches 313 K. The top of the bed (Z=0.993) reaches a temperature of 315.2 K.

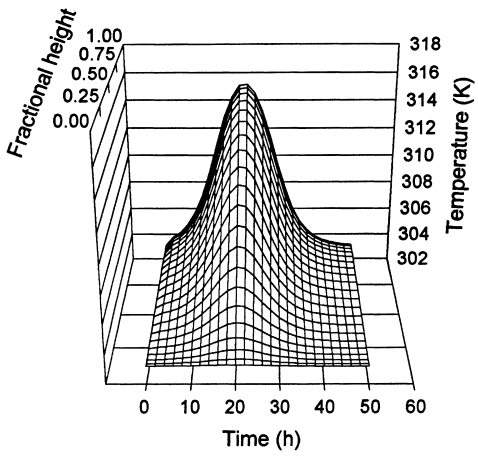

Fig. 3. Predicted temperature profiles during an unmixed fermentation with *Rhizopus oligosporus* with aeration from the bottom throughout (i.e. normal packed bed operation), using the parameters in Table 1. Note how the axial temperature profile in the bed changes with time.

From this point onwards, the use of a bed without mixing but with forced aeration from the bottom throughout the fermentation will be referred to as "normal" operation. With such operation, over short time periods of an hour or less, the bed can be considered to be in a pseudosteady state, because the temperature gradient along the bed changes only relatively slowly with time, especially relative to the changes caused by air reversal and mixing. This temperature gradient will be referred to below as the "pseudosteady gradient". In fact, if the growth rate remained constant, then a true steady state would be reached for normal operation, with a stable temperature profile established along the height of the bed.

Strategies to prevent overheating, such as cooling the inlet air, increasing the superficial velocity and changing the bioreactor height to diameter ratio have already been investigated [6]. The investigations below will determine whether frequent reversal of the direction of airflow, or frequent mixing can help to prevent the critical temperature from being exceeded.

3.3. Air reversal as a strategy to prevent overheating

If a packed bed has been chosen because the substrate cannot be mixed due to deleterious effects on the microbe, then air reversal can be tried. The logic behind air reversal is that, upon switching of the air direction, the hot end of the column is in contact with cool air, and therefore cools down. In this way it should be possible to prevent the ends of the column from ever exceeding the critical temperature.

Air reversal could be done in either of two ways. The direction of airflow could be reversed, or alternatively, the whole column could be inverted. However, changing the direction of the airflow is simpler, and the analysis assumes that this is done. In addition, two strategies might be used to trigger the reversal of airflow. A thermocouple could be inserted at either end of the bed, with the airflow being reversed whenever the temperature measured by the thermocouple at the air outlet end reached the critical temperature. Alternatively, the direction of airflow could be reversed on a regular basis, and this is done for the current simulation work.

The initial simulation uses a period of 1 h between air reversal events. This is much longer than the characteristic heating time and therefore should have little effect on the maximum temperature reached. However, this analysis shows the underlying behaviour of an individual air reversal event because it allows sufficient time between air reversal events for the re-establishment of the pseudosteady temperature gradient.

Fig. 4 shows the temperature profile at the top of the column (Z=0.993) during the fermentation. Due to the air reversal, the bottom of the column is in contact with the inlet air for 1 h and the top of the column is in contact with it for the next hour. As expected, the top of the column is maintained at the inlet air temperature when it is in contact

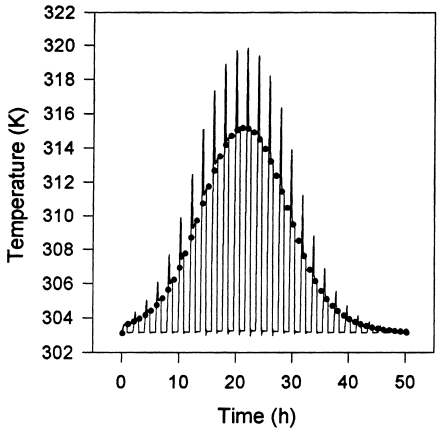

Fig. 4. Predicted temperature profile at the top of the packed bed (Z=0.993) for a fermentation during which the direction of airflow is reversed hourly. All other parameters and operating conditions are as in Table 1. The profile for normal operation (no air reversals), indicated by the solid circles, is provided for comparison.

with the inlet air. Furthermore, the average temperature experienced by the microbe at the top of the column is lower than the temperature experienced during normal operation. However, the top of the column actually exceeds the temperature for normal operation for short periods of time. A maximum temperature of 319.8 occurs at 21.1 h at the top of the column for the hourly air reversal compared to the maximum temperature of 315.2 K for normal operation. This behaviour can be explained by focusing on an individual mixing event (Fig. 5), in which the air is switched from entering at the bottom of the column to entering at the top of the column.

Immediately before an air reversal event, while the air is still passing up from the bottom of the column, the top is hot and the bottom is cool. After the air reversal the top quickly cools to the inlet air temperature, because the temperature front caused by the reversal of airflow passes the top within 2 min. During this period the rest of the column heats up because the air is preheated at the top of the column and therefore does not remove the energy released by microbial metabolism in the remainder of the column. In fact, since the air is hotter than the lower regions of the column, it actually contributes to the warming in these regions. As a result, at the time of the peak growth rate, immediately after the airflow is switched to the top of the column, the heating rate at the bottom of the column is about 0.9 K min^{-1}. This is a higher than the maximum rate of 0.4 K min^{-1} calculated for microbial metabolism alone.

As the front reaches a collocation point, that point begins to cool, but the points below it continue to heat. This appears in Fig. 5(a) as a progression of temperature peaks, each reaching a higher temperature. It takes almost half an hour for the front to reach the bottom of the column, and by this time the temperature at the bottom has exceeded the temperature for normal operation. The temperature gradient behind the front corresponds to the pseudosteady gradient,

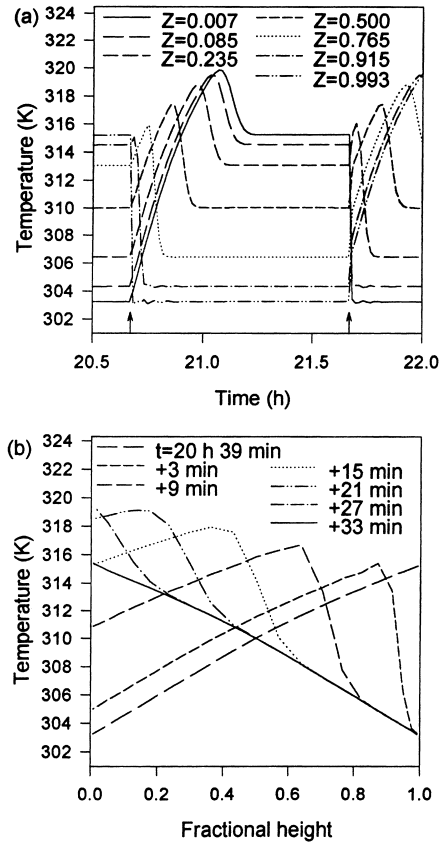

Fig. 5. Detail of temperature profiles during one air reversal event during the fermentation shown in Fig. 4. Arrows indicate times of air reversals. (a) Temperature versus time at various fractional heights. The first air reversal event corresponds to a switch of aeration from the bottom to the top of the column. (b) Temperature versus fractional height for several times after the air reversal at 20 h and 39 min. During this period the air is blown into the top of the column, which corresponds to a right to left direction across the graph.

although in the reverse direction because the aeration is from top to bottom. Fig. 5(b) shows the same phenomenon from a different perspective. After the air reversal, the front can be seen travelling down the column (i.e. from right to left across the figure).

Fig. 6(a) shows the detail of two air reversal events for the case where the direction of the airflow is reversed every 5 min. The first event corresponds to a switch of aeration from the bottom to the top and the second corresponds to a switch of aeration back to the bottom. Sufficient time is not allowed between switching events for the full cycle shown in Fig. 5(a) to occur. As a result, the profiles appear quite different. At most collocation points, there is a cyclic fluctuation in temperature, with the amplitude being greatest near the ends of the column. Most noticeably, the middle of the column remains near the maximum temperature for growth (325 K). This occurs because the front never reaches this location. After the first air reversal the front does not reach collocation points 2,5 and 8 (Z=0.007, 0.085 and 0.235, respectively); these are at the far end from the air inlet during this period. Therefore, these points heat throughout

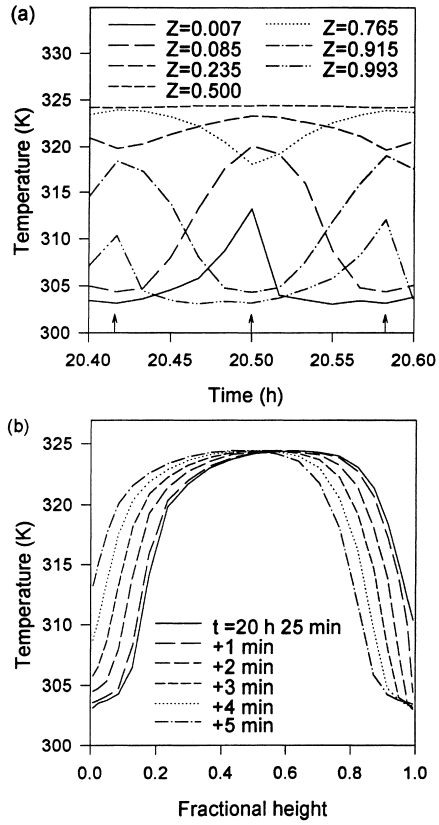

Fig. 6. Detail of predicted temperature profiles for a fermentation during which the direction of airflow is reversed every 5 min. All other parameters and operating conditions are as in Table 1. (a) Temperature versus time at various fractional heights. Arrows indicate times of air reversals. (b) Temperature versus fractional height for several times after the air reversal at 20 h and 25 min, until just before the next air reversal 5 min later. During this period the air is blown into the top of the column, which corresponds to a right to left direction across the graph.

this period. The front quickly passes points 22 and 19 (Z=0.993 and 0.915, respectively), since these are now close to the air inlet, and these points cool rapidly to the pseudosteady temperatures. The front only reaches point 16 (Z=0.765) for a short period, and it does not pass all the way past this point before the airflow is reversed, therefore point 16 cools only slightly before the next reversal of airflow.

The temperature versus distance plot (Fig. 6(b)) shows some of this behaviour more clearly, for the period between two switching events, with the airflow coming from the top of the column. The front moves into the column (travelling from right to left in Fig. 6(b)) and the region to the left heats up because it is not being effectively cooled. By the time of the next switching event 5 min later the front has only travelled part way down the column. As a result, significant temperature fluctuations occur only in the quarter of the column near the top and the quarter near the bottom.

3.4. Mixing as a strategy to prevent overheating

The above analysis indicates that air reversal is not a good strategy for preventing overheating. On the other hand, discontinuous mixing has been successful in a number of applications [20–22], although it can only be used where the disruption of the microorganism and substrate can be tolerated. In the current work it is assumed that a screw agitator is inserted vertically in the bed and is activated at regular intervals [20,21]. Fig. 7 shows the predicted temperature profiles at the top of the bed (Z=0.993), for a column in which aeration is always from the bottom, but which is mixed hourly. Again, this enables the underlying behaviour of individual mixing events to be discerned. As with air reversal, the maximum temperature exceeds that obtained during normal operation. However, as a result of the long intervals between mixing events, the underlying temperature profile is quite similar to that for normal operation.

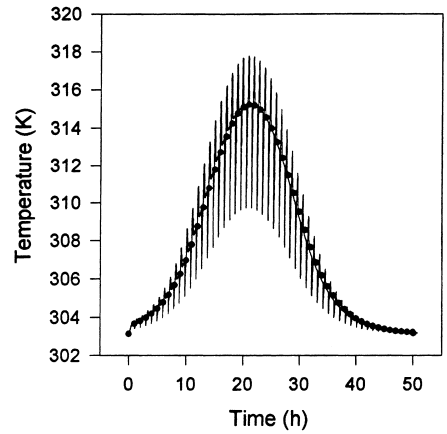

Fig. 7. Predicted temperature profile at the top of the packed bed (Z=0.993) for a fermentation during which the column contents are mixed hourly. All other parameters and operating conditions are as in Table 1. The profile for normal operation (no mixing), indicated by the solid circles, is provided for comparison.

Fig. 8(a) shows one mixing event in more detail. Immediately upon mixing, the whole column is at the same temperature. As the front travels up the column, each collocation point is cooled in turn. Points above the temperature front increase in temperature due to the release of waste metabolic heat. As is the case with air reversal, it takes a long time (22 min), for the front to reach the top of the column and by that time the waste metabolic heat has raised the temperature to 317.8 K. This is well above the pseudosteady temperature at the top for normal operation (315.2 K).

The heating rate at the top of the column immediately after mixing is 0.43 K min^{-1}, approximately, what would be expected for heating by microbial waste heat production. Fig. 8(b) shows why this is the case. Immediately after mixing, the column temperature is uniformly at 310 K. As the air enters the newly mixed column, it quickly heats up to 310 K, and therefore neither heats nor cools the remainder of the column, which therefore heats solely due to microbial waste heat production. This contrasts with the air reversal situation, in which the heating rate at the far end of the

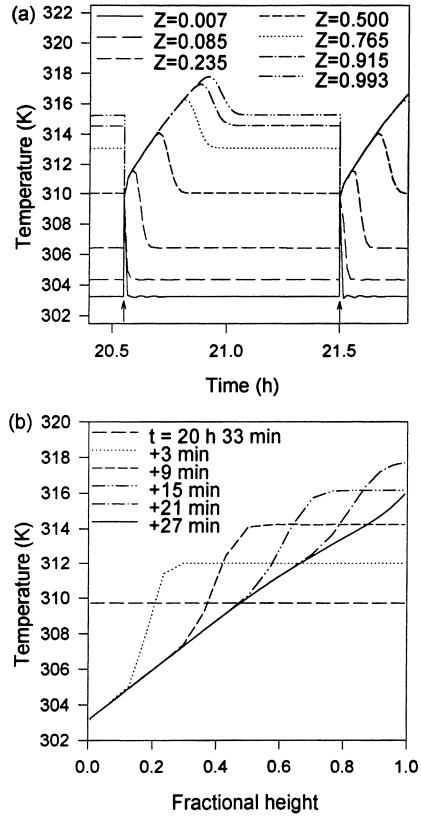

Fig. 8. Detail of predicted temperature profiles during one mixing event during the fermentation shown in Fig. 7. (a) Temperature versus time at various fractional heights. Arrows indicate times of mixing events. (b) Temperature versus fractional height for several times after the mixing event at 20 h and 33 min.

column immediately after an air reversal was greater than that expected for microbial growth alone.

Fig. 9 shows one mixing event for a bed which is mixed every 5 min. Note that in this situation the maximum temperature in the bed of 314.4 K is lower than the maximum temperature of 315.2 K obtained during normal operation, indicating that mixing can help to reduce the maximum temperature obtained in a packed bed bioreactor. Fig. 9 shows an underlying behaviour quite similar to that for the hourly mixing, except that the next mixing event occurs before the temperature has risen above the pseudosteady value for normal operation.

Fig. 9 indicates why frequent mixing reduces the maximum temperature attained. Convection cools the bottom of the column much faster than the rest of the column heats up (compare the curves for Z=0.085 and below with the curve for Z=0.235 and above). The frequent mixing events regularly distribute this cool material throughout the column, cooling the top faster than is possible with air convection alone, since in an unmixed column the air must cool the rest of the column before it can begin to cool the top (see Fig. 2). Infrequent mixing is not successful because it allows sufficient time for the front behaviour shown in Fig. 8 to occur.

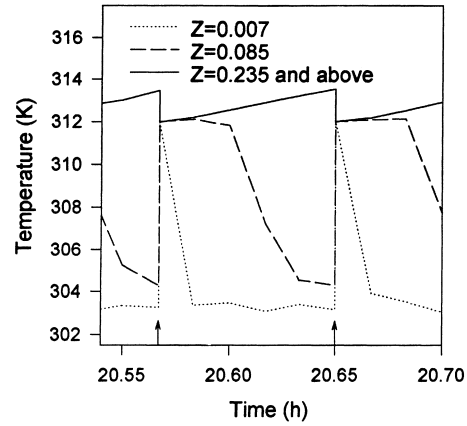

Fig. 9. Detail of predicted temperature profiles for a fermentation during which the column contents are mixed every 5 min. Arrows indicate times of mixing events. Profiles are shown for various fractional heights, although there is no difference in the profiles for fractional heights of 0.235 and above. All other parameters and operating conditions are as in Table 1.

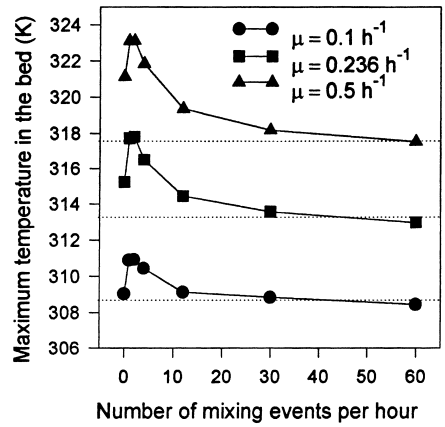

Fig. 10. Predicted effect of mixing frequency on the maximum temperature obtained in a packed bed, shown for three different values of the maximum specific growth rate (μ_{gopt}). All other parameters and operating conditions are as in Table 1. The maximum temperatures for the well-mixed system were 308.7, 313.3 and 317.6 K (indicated by the dotted lines) for the specific growth rates of 0.1, 0.236 and 0.5 h^{-1}, respectively.

3.5. *Exploring the potential of mixing to enable adequate temperature control*

The previous section showed that mixing can decrease the maximum temperature observed in the packed bed compared to normal operation. Fig. 10 shows the effect of mixing frequency on the maximum temperature obtained in the bed. Plots are given for three values of μ_{gopt}, since a wide range of specific growth rates might be expected in SSF with different organisms [7]. As noted previously, at relatively low mixing frequencies, the maximum temperature achieved during the fermentation actually exceeds that for normal operation (zero mixing events per hour). However, at high mixing frequencies, of the order of 10–60 mixing events per hour, depending on the specific growth rate, the maximum temperature obtained is lower than that

for normal operation. The benefits of mixing, namely the degree of reduction in the maximum temperature attained, increase with increasing specific growth rate.

At mixing frequencies of 30–60 mixing events per hour, the predicted maximum temperatures are very close to the maximums predicted for perfectly mixed beds, suggesting that there is no advantage of having continuous mixing in SSF processes. Therefore, stirred beds can be relatively long and fitted with travelling agitators, as has been done for two pilot scale bioreactors [20,21]. These travelling agitators will intermittently mix each location in the bed. The bed length and speed of agitator travel must be coordinated to enable sufficiently frequent mixing at all points.

Of course, the mixing frequencies required to prevent excessive temperature rises will also depend on the superficial velocity and the bed height. The model used in the current work can be used to explore the interrelationship between these variables. However, the practical and economical limits on superficial velocities in packed beds have not yet been determined, so this analysis is not done here.

3.6. Possible improvements to the model

Several improvements may be appropriate for the model. Firstly, when either the direction of airflow is reversed or the substrate bed is mixed, there is a large difference in temperature between the substrate at the inlet air end of the column and the incoming air. Therefore, the assumption of thermal equilibrium between the air and the substrate in the current model may not be appropriate for part of the column for part of the time. Instead a driving force model for both heat transfer and evaporation might be needed to accurately describe the period soon after mixing or air reversal. Secondly, it is desirable to incorporate a better description of what happens during mixing. The model currently simulates mixing as an instantaneous redistribution of energy and biomass. However, mixing actually occurs over a finite period and it is quite possible that mixing leads to more effective cooling than was modelled in the present work. De Reu et al. [22] had a finite mixing period in their discontinuously rotated drum, and noted that the temperature actually fell during the rotation period.

4. Conclusions

Two main conclusions can be drawn from this work: a specific conclusion about strategies for preventing overheating in packed bed bioreactors, and a general conclusion about strategies for investigating the design and operation of bioreactors for SSF.

Firstly, the model suggests that periodic air reversal is not a useful strategy for preventing overheating during SSF in packed bed bioreactors. However, if mixing can be reasonably tolerated by the microorganism, then frequent mixing events, of the order of 10–60 mixing events per hour, can decrease the maximum temperature attained in the packed bed. The model also provides an understanding, on the basis of heat transfer dynamics, as to why mixing is successful and air reversal is not.

Secondly, this work demonstrates that modelling is essential for the design of effective large-scale bioreactors for SSF. There is no evidence in the literature that models have actually been used to do this. Models can be used to evaluate design and operational strategies rapidly, identifying those with the greatest potential to overcome overheating problems, and eliminating ideas which seem promising but in fact have no or poor potential. The modelling approach is more cost effective than evaluating these strategies solely by experiments in large-scale bioreactors. Of course the most fruitful approach will be to run simultaneous modelling and experimental programs.

5. Nomenclature

b	sensitivity of growth kinetics to increase in temperature (K)
C_{pa}	heat capacity of moist air (J kg^{-1} K^{-1})
C_{pb}	heat capacity of bed (J kg^{-1} K^{-1})
C_{ps}	heat capacity of substrate (J kg^{-1} K^{-1})
f	water carrying capacity of air (kg kg^{-1} K^{-1})
H	overall bed height (m)
i	subscript denoting the value is at the ith collocation point
k_a	thermal conductivity of moist air (W m^{-1} K^{-1})
k_b	thermal conductivity of the bed (W m^{-1} K^{-1})
k_s	thermal conductivity of the substrate (W m^{-1} K^{-1})
n	number of internal collocation points
Q_{gen}	maximum rate of heat generation due to growth (J s^{-1} m^{-3})
Q_{heat}	heating rate at maximum heat generation rate (K s^{-1})
t	fermentation time (s)
T	bed temperature (K)
T_a	temperature of inlet air (K)
T_0	initial bed temperature (K)
T_{avg}	average temperature after a mixing event (K)
T_{max}	maximum temperature for growth (K)
T_{opt}	optimum temperature for growth (K)
v_z	superficial velocity (m s^{-1})
X	biomass concentration (kg kg^{-1})
X_m	maximum biomass concentration (kg kg^{-1})
X_0	initial biomass (kg kg^{-1})
Y	metabolic heat yield coefficient (J kg^{-1})
z	axial position (m)
Z	fractional axial position (z/H)

Greek letters

ε	void fraction
λ	enthalpy of vapourization of water (J kg^{-1})
μ_g	specific growth rate (s^{-1})

μ_{gopt} specific growth rate at the optimum temperature (s^{-1})
ρ_a density of moist air (kg m^{-3})
ρ_b density of bed (kg m^{-3})
ρ_s density of substrate (kg m^{-3})

References

[1] B.K. Lonsane, G. Saucedo-Castaneda, M. Raimbault, S. Roussos, G. Viniegra-Gonzalez, N.P. Ghildyal, M. Ramakrishna, M.M. Krishnaiah, Scale-up strategies for solid state fermentation systems, Process. Biochem. 27 (1992) 259–273.
[2] M.V. Ramana Murthy, N.G. Karanth, K.S.M.S. Raghava Rao, Biochemical engineering aspects of solid-state fermentation, Adv. Appl. Microbiol. 38 (1993) 99–147.
[3] K.S.M.S. Ragheva Rao, M.K. Gowthaman, N.P. Ghildyal, N.G. Karanth, A mathematical model for solid state fermentation in tray bioreactors, Bioprocess Eng. 8 (1993) 255–262.
[4] S. Rajagopalan, J.M. Modak, Heat and mass transfer simulation studies for solid-state fermentation processes, Chem. Eng. Sci. 49 (1994) 2187–2193.
[5] N.P. Ghildyal, M.K. Gowthaman, K.S.M.S. Raghava Rao, N.G. Karanth, Interaction between transport resistances with biochemical reaction in packed bed solid-state fermentors: effect of temperature gradients, Enzyme Microb. Technol. 16 (1994) 253–257.
[6] P. Sangsurasak, D.A. Mitchell, Incorporation of death kinetics into a 2D dynamic heat transfer model for solid state fermentation, J. Chem. Technol. Biotechnol. 64 (1995) 253–260.
[7] P. Sangsurasak, D.A. Mitchell, Validation of a model describing 2-dimensional heat transfer during solid state fermentation in packed bed bioreactors, Biotechnol. Bioeng. (1998), in press.
[8] G. Saucedo-Casteneda, M. Gutierrez-Rojas, G. Bacquet, M. Raimbault, G. Viniegra-Gonzalez, Heat transfer simulation in solid substrate fermentation, Biotechnol. Bioeng. 35 (1990) 802–808.
[9] D.M. Himmelblau, Basic Principles and Calculations in Chemical Engineering. 5th ed., Prentice-Hall, Englewood Cliffs, NJ, 1982.
[10] V.E. Sweat, Thermal properties of foods, in: M.A. Rao, S.S. Rizvi (Eds.), Engineering Properties of Foods, Marcel Dekker, New York, 1986, pp. 49–132.
[11] R.H. Perry, D.W. Green, J.O. Maloney, Perry's Chemical Engineer's Handbook, 6th ed., McGraw-Hill, New York, 1984.
[12] J.J.C. Van Lier, J.T. Van Ginkel, G. Straatsma, J.P.G. Gerrits, L.J.L.D. Van Griensven, Composting of mushroom substrate in a fermentation tunnel: compost parameters and a mathematical model, Netherlands J. Agri. Sci. 42 (1994) 271–292.
[13] K.W. Szewczyk, L. Myszka, The effect of temperature on the growth of *A. Niger* in solid state fermentation, Bioprocess Eng. 10 (1994) 123–126.
[14] E. Gumbira-Sa'id, D.A. Mitchell, P.F. Greenfield, H.W. Doelle, A packed bed solid-state fermentation system for the production of animal feed: Cultivation, drying and product quality, Biotechnol. Lett. 14 (1992) 623–628.
[15] M.S. Terzic, M.S. Todorovic, The experimental investigation of isothermal and nonisothermal fluid flow and heat transfer through porous media, in: M. Quintard, M. Todorovic (Eds.), Heat and Mass Transfer in Porous Media, Elsevier, Amsterdam, 1992, pp. 585–600.
[16] R.C. Weast, Handbook of Chemistry and Physics, 55th ed., CRC Press, OH, 1974.
[17] J. Villadsen, M.L. Michelsen, Solution of Differential Equation Models by Polynomial Approximation, Prentice-Hall, NJ, 1978.
[18] B.A. Finlayson, Nonlinear Analysis in Chemical Engineering, McGraw-Hill, New York, 1980.
[19] A.C. Hindmash, GEAR: ordinary differential equation system solver, Lawrence Livermore Laboratory Report UCID-30001, Rev. 3. 1974.
[20] A. Durand, D. Chereau, A new pilot reactor for solid-state fermentation: Application to the protein enrichment of sugar beet pulp, Biotechnol. Bioeng. 31 (1988) 476–486.
[21] M. Xue, D. Liu, H. Zhang, Q. Hongyan, Z. Lei, A pilot process of solid state fermentation from sugar beet pulp for the production of microbial protein, J. Ferment. Bioeng. 73 (1992) 203–205.
[22] J.C. De Reu, M.H. Zwietering, F.M. Rombouts, M.J.R. Nout, Temperature control in solid substrate fermentation through discontinuous rotation, Appl. Microbiol. Biotechnol. 40 (1993) 261–265.